

RESEARCH ARTICLE

Metastases to the parotid nodes: CT and MR imaging findings

¹Nobuo Kashiwagi, ¹Takamichi Murakami, ²Masafumi Toguchi, ³Katsuyuki Nakanishi, ¹Shojiro Hidaka, ¹Hideyuki Fukui, ⁴Masatomo Kimura, ⁵Mutsukazu Kitano and ⁶Noriyuki Tomiyama

¹Department of Radiology, Kindai University Faculty of Medicine, Osaka, Japan; ²Department of Radiology, Ryukyus University Faculty of Medicine, Okinawa, Japan; ³Department of Diagnostic Radiology, Osaka Medical Center for Cancer and Cardiovascular Diseases, Osaka, Japan; ⁴Department of Pathology, Kindai University Faculty of Medicine, Osaka, Japan; ⁵Department of Otolaryngology, Kindai University Faculty of Medicine, Osaka, Japan; ⁶Department of Diagnostic and Interventional Radiology, Osaka University Graduate School of Medicine, Osaka, Japan

Objectives: To present and characterize CT and MR imaging findings of metastases to the parotid nodes.

Methods: CT ($n = 10$) and MR ($n = 11$) images from 14 patients with metastases to the parotid nodes were reviewed. The primary tumour sites were the ocular adnexa in five patients, facial skin in four patients, upper aerodigestive tract in four patients and thyroid gland in one patient. CT and MR images were evaluated with emphasis on the size and number of parotid tumours, their location in the parotid gland, the presence of associated clinically pathological cervical nodes or previous history of cervical node metastasis, margin characteristics and the presence of central necrosis.

Results: A total of 18 tumours were identified in 14 patients, with an average maximal cross-sectional diameter of 19 mm (7–44 mm). 12 patients had a single parotid tumour and 2 patients had unilateral multiple tumours; 12 tumours in 10 patients were located in the parotid tail, 6 tumours in 4 patients were located in the superficial lobe and no tumour was noted in the deep lobe. In the superficial lobe, four of six tumours were located in the pretragal area. Three of nine patients whose primary sites were the ocular adnexa or skin had associated clinically pathological cervical nodes. None of these patients had a previous history of cervical node metastasis. All five patients with other primary sites had associated pathological cervical nodes or a history of such. 11 tumours had well-defined margins and 7 tumours had ill-defined margins. Post-contrast images showed central necrosis in 2 of 11 tumours.

Conclusions: Metastases to the parotid nodes tend to present as solitary parotid masses with two preferential sites.

Dentomaxillofacial Radiology (2016) **45**, 20160201. doi: 10.1259/dmfr.20160201

Cite this article as: Kashiwagi N, Murakami T, Toguchi M, Nakanishi K, Hidaka S, Fukui H, et al. Metastases to the parotid nodes: CT and MR imaging findings. *Dentomaxillofac Radiol* 2016; **45**: 20160201.

Keywords: CT; MRI; parotid gland; metastasis

Introduction

Among the salivary glands, only the parotid gland contains lymph nodes and therefore, lymphatic metastatic tumours and Warthin's tumours arise almost invariably in the parotid gland. In contrast to Warthin's tumours,

which are the second most common parotid tumour, lymphatic metastatic tumours to the parotid gland are relatively rare.^{1–4} Thus far, the imaging features of these tumours have not been well characterized. The present study analyzed CT and MR imaging findings from 14 patients with metastases to the parotid nodes.

Methods and materials

Patients

We retrospectively reviewed the CT and MR images of 14 consecutive patients who had been diagnosed with metastases to the parotid nodes at 2 referral centres for head and neck tumours in Japan between 2004 and 2015. The patients were seven males and seven females with a mean age of 78 years (range, 61–97 years). The primary tumour sites were the ocular adnexa in five patients (four in the eyelid and one in the lacrimal sac), facial skin in four patients (three in the cheek and one in the temple), upper aerodigestive tract in four patients (two in the larynx, one in the oral cavity and one in the maxillary sinus) and thyroid gland in one patient. The diagnosis of metastases to the parotid nodes was made by surgical resection in 11 patients. In the remaining three patients, it was made by fine-needle aspiration cytology because of deterioration of the patient general condition or the patient refusal of surgery. The histological tumour types were squamous cell carcinoma in six patients, sebaceous cell carcinoma in four patients, Merkel cell carcinoma in two patients and malignant melanoma and papillary adenocarcinoma in one patient each.

Imaging

CT and MRI were performed in 10 and 11 patients, respectively, with 7 patients undergoing both CT and MR examinations. All CT images were obtained as 5.0-mm axial CT images with a soft-tissue algorithm using various CT scanner models. Three patients underwent plain CT scanning, five patients underwent contrast-enhanced CT scanning and two patients underwent both plain and contrast-enhanced CT scanning. MR images were obtained using a 1.5-T magnet in nine patients and a 3.0-T magnet in two patients. In all patients, we obtained axial spin-echo T_1 weighted, fast spin-echo T_2 weighted and short-inversion-time inversion-recovery images. In nine patients, coronal T_1 weighted, T_2 weighted or short-inversion-time inversion-recovery images were obtained. In nine patients, axial and coronal post-contrast T_1 weighted images were obtained. The section thickness was 4–5 mm, and the range of pixel size was from 0.4×0.5 to 0.9×1.0 mm.

Data analysis

Two experienced radiologists reviewed all CT and MR images in consensus with particular attention to the following points: the size and number of parotid tumours, their location in the parotid gland, the presence of associated clinically pathological cervical nodes or previous history of cervical node metastasis, margin characteristics and the presence of central necrosis. Size was measured as the maximal diameter in the axial section and defined as pathological when it exceeded 6 mm, based on the morphological study of normal parotid lymph nodes.⁵ The tumour location in the parotid gland was categorized into three areas: superficial

lobe, deep lobe and parotid tail. The superficial lobe was defined as an area lateral to the retromandibular vein, the deep lobe was defined as an area medial to the retromandibular vein and the tail was defined as the inferior 2.0 cm area of the gland.⁶ The cervical node was defined as clinically pathological when it had a minimal axial diameter of >10 mm or central necrosis. Margin characteristics were classified as well or ill (coexistence of defined and ill-defined margins was defined as an ill-defined margin). Central necrosis was defined as ring enhancement in post-contrast images.

Results

The clinical information and CT and MR imaging findings are summarized in Table 1, and these representative images are provided in Figures 1–3. Among 14 patients, a total of 18 tumours were identified, with an average maximal cross-sectional diameter of 19 mm (7–44 mm). 12 patients had a single parotid tumour and 2 patients had unilateral multiple tumours. With respect to tumour locations in the parotid gland, 12 tumours in 10 patients were located in the parotid tail, 6 tumours in 4 patients were located in the superficial lobe and no tumour was noted in the deep lobe. Among the six tumours in the superficial lobes, four tumours were located in the pretragal area. 5 of the 14 patients had clinically pathological cervical nodes. Among nine patients in whom the primary sites were the skin or ocular adnexa, only three patients had clinically pathological cervical nodes and none had a previous history of cervical node metastasis. In contrast, all five patients in whom the primary sites were the upper aerodigestive tract or thyroid had clinically pathological cervical nodes or previous history of neck dissection due to cervical node metastasis. 11 tumours had well-defined margins and 7 tumours had ill-defined margins. Among 9 patients who underwent contrast-enhanced imaging, 2 of 11 tumours had central necrosis.

Discussion

Secondary neoplastic involvement of the parotid gland can arise from regional (supraclavicular) and distant (infraclavicular) primary neoplasms. Supraclavicular neoplasms account for over 90% of metastatic tumours to the parotid gland and such metastases are thought to occur *via* lymphatic spread to the parotid lymph nodes.^{7–9} The criterion for clinical parotid lymph node metastasis has been the presence of a palpable parotid lesion based on manipulation,^{7,10,11} and there are no diagnostic criteria based on imaging studies. Therefore, in this study, we provisionally defined the parotid lymph node to be clinically pathological when its maximal diameter exceeded 6 mm, based on a previous anatomic study that described the mean maximal diameter of normal parotid nodes as 3.7 mm (range, 2–6 mm) in the

Table 1 Patients' characteristics and imaging findings

Case number	Age (years)/sex	Obtained images	Primary site	Histology	Size (mm)	Number of parotid lesions	Location in the parotid gland	Associated pathological lymph nodes	History of cervical node metastasis	Margin characteristics	Necrosis
1	75/F	CECT	Eyelid	Sebaceous cell carcinoma	38	1	Superficial lobe	None	None	Well defined	Present
2	90/M	CT, MRI	Skin (temple)	Squamous cell carcinoma	20, 7, 8	3	Superficial lobe in all	Present	None	Ill defined in one, well defined in two	N/A
3	89/M	CT, MRI	Skin (cheek)	Squamous cell carcinoma	21	1	Superficial lobe	None	None	Ill defined	N/A
4	71/F	CECT, MRI	Eyelid	Sebaceous cell carcinoma	25	1	Superficial lobe	None	None	Ill defined	None
5	72/F	CE-MRI	Eyelid	Sebaceous cell carcinoma	24	1	Tail	Present	None	Well defined	None
6	61/M	CECT, MRI	Lacrimal sac	Malignant Melanoma	10	1	Tail	None	None	Ill defined	None
7	85/F	CE-MRI	Skin (cheek)	Merkel cell carcinoma	16	1	Tail	None	None	Well defined	None
8	97/F	CT	Eyelid	Sebaceous cell carcinoma	23	1	Tail	None	None	Well defined	N/A
9	90/F	MRI	Skin (cheek)	Merkel cell carcinoma	13	1	Tail	Present	None	Well defined	N/A
10	69/M	CECT, MRI	Oral cavity	Squamous cell carcinoma	35	1	Tail	None	Present	Ill defined	None
11	70/M	CECT, CE-MRI	Larynx	Squamous cell carcinoma	8, 8, 12	3	Tail in all	Present	Present	Well defined in all	None
12	74/M	CECT	Larynx	Squamous cell carcinoma	24	1	Tail	Present	Present	Ill defined	Present
13	76/F	CECT, CE-MRI	Thyroid	Papillary adenocarcinoma	44	1	Tail	Present	None	Ill defined	None
14	73/M	MRI	Maxillary sinus	Squamous cell carcinoma	16	1	Tail	None	Present	Well defined	N/A

CECT, contrast-enhanced CT; F, female; M, male; N/A, not applicable.

superficial lobe and 2.8 mm (range, 2–6 mm) in the deep lobe.⁵ Although no occult metastases or false-positive nodes were found in our patients who underwent parotidectomy, further studies to determine the criteria for clinically pathological parotid nodes are needed.

Previous radiologic literature has described a tendency for metastases to the parotid nodes to be multifocal.^{12,13} In contrast, dermatologic and otolaryngologic studies have reported that metastases to the parotid nodes usually appear as solitary parotid masses.^{10,14} Indeed, the



Figure 1 A 71-year-old female with metastasis to the parotid node from sebaceous cell carcinoma of the eyelid: (a) an axial post-contrast CT image is showing a homogeneous enhancing tumour in front of the tragus in the superficial lobe. (b, c) T_1 weighted (b) and T_2 weighted (c) MR images are showing an ill-defined tumour in front of the tragus in the superficial lobe. The signal intensity of the tumour is equal to that of muscle on the T_1 weighted image and slightly higher than that of the muscle on the T_2 weighted image.

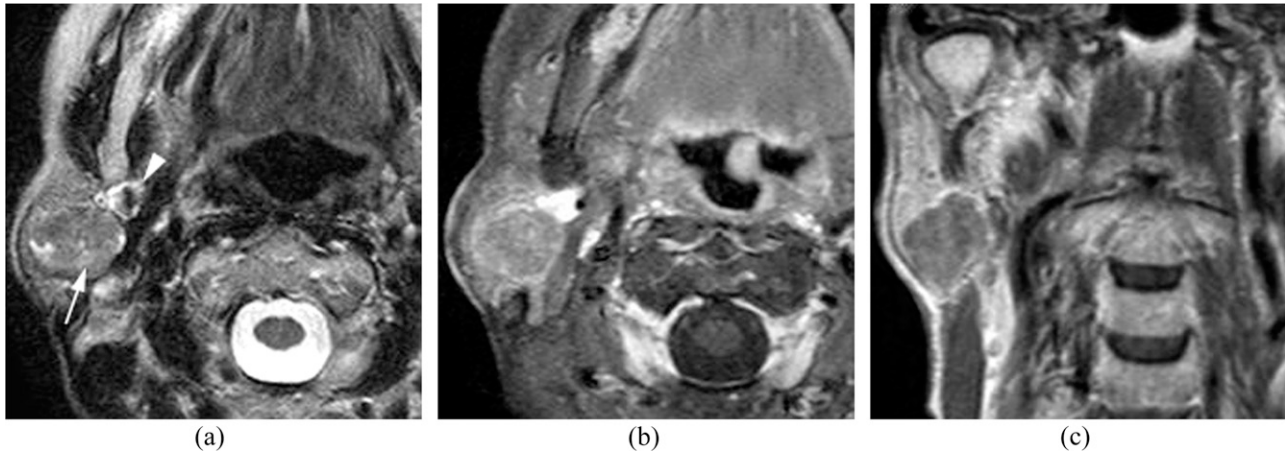


Figure 2 A 72-year-old female with metastasis to the parotid node from sebaceous cell carcinoma of the eyelid: (a) an axial T_2 weighted image is showing a well-defined mass in the parotid tail (arrow). The arrowhead is indicating the retromandibular vein. (b, c) On contrast-enhanced fat-suppressed T_1 weighted axial (b) and coronal (c) images, the mass is showing slight enhancement.

majority of our cases (12 of 14 cases) presented with a solitary parotid tumour. Although further studies with larger number of cases may be needed, radiologists should be aware that a solitary parotid lesion does not eliminate the possibility of metastasis to the parotid node.

In our study, metastases to the parotid nodes were most frequently noted in the parotid tail, followed by the pretragal area in the superficial lobe, which corresponds well to the distribution of the parotid lymph nodes. The parotid space harbours both intraglandular and extraglandular lymph nodes, and both groups are considered as the parotid nodes.^{7,10} The aggregated total number of parotid nodes ranges from 20 to 30, of which 8–10 parotid nodes are intraglandular.^{11,15–17} The intraglandular lymph nodes exist along the course of the retromandibular vein and are predominantly located in the parotid tail.^{11,12,15} Further, a total of 6–9 intraglandular lymph nodes exist in the superficial lobe and

1–2 nodes in the deep lobe. Extraglandular nodes are located mainly in front of the tragus, followed by around the parotid tail.^{10,15}

Our results concerning the associated clinically pathological cervical nodes appeared to be consistent with previously reported lymphatic drainage patterns of the cutaneous area of the head and neck.^{4,11,18–20} The parotid lymph nodes drain a large part of the cutaneous area of the head and neck. Lymph drainage from the ocular adnexa, forehead and the lateral aspect of the head is first drained to the parotid nodes and subsequently to the upper cervical nodes, such as the external jugular nodes and Level 2 nodes. This lymphatic drainage pattern reflects the result that two-thirds of the patients in whom the primary sites were the ocular adnexa and facial skin showed no involvement of pathological cervical nodes. In contrast, all the patients in whom the primary sites were the upper aerodigestive

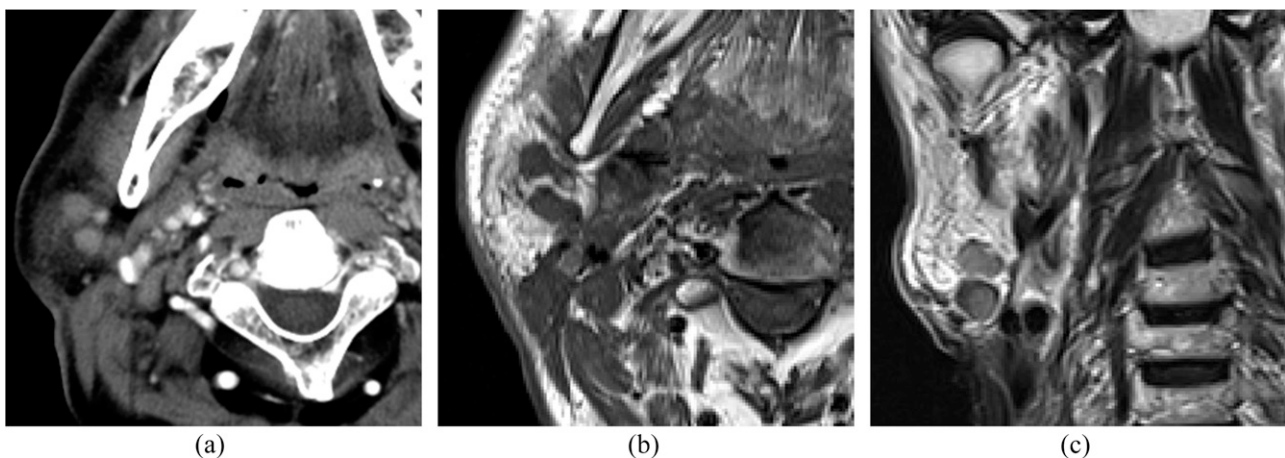


Figure 3 A 70-year-old male with metastases to the parotid nodes from squamous cell carcinoma of the larynx: (a) an axial post-contrast CT image is showing multiple homogeneous enhancing masses in the parotid tail. (b, c) Axial T_1 weighted (b) and coronal T_2 weighted (c) images are showing multiple well-defined masses in the parotid tail.

tract and thyroid gland had associated pathological cervical nodes or previous history of neck dissection for cervical node metastasis. This suggests that metastases to the parotid nodes from these carcinomas seem to be the result of extensive lymph node spread or changes in the normal pathways of lymph node spread due to prior surgical procedures.^{21–23}

Identical to previous reports,^{12–14} our study showed that metastases to the parotid nodes can have an either ill-defined or well-defined margin and occasionally have central necrosis. An ill-defined margin in cervical node metastases from head and neck cancer is a highly specific sign of extracapsular tumour spread, which is predictive of poor prognosis.^{24,25} Central necrosis in cervical lymph node metastases is also reported to be a predictor of extracapsular spread.^{25,26} Regardless of whether an ill-defined margin and central necrosis predict poor prognosis in metastases to the parotid nodes, radiologists should be aware that they can have varied margin characteristics and occasionally have central necrosis.

The present study provided only non-specific CT and MR findings for metastases to the parotid nodes, and these findings overlap with the findings for a number of primary benign and malignant tumours. However, the

predilection site might provide a clue for diagnosing metastases to the parotid nodes; the main differential diagnosis for such lesions appears to be Warthin's tumours, which also tend to occur in the parotid tail.^{27,28} With regard to their differentiation, the presence of an ill-defined margin or central necrosis suggests a diagnosis of metastases to the parotid nodes, and bilateral parotid lesions or intratumoral cystic components with an eccentric location suggest a diagnosis of Warthin's tumours.^{28,29}

This study has several limitations. First, the small patient populations and retrospective nature of the study do not allow any conclusion to be drawn about the differentiation between metastatic parotid tumours and primary parotid tumours. Second, confirmation by pathological examination in the resected specimens was not performed in all cases, and occult metastases in the parotid deep lobe and cervical lymph nodes were not evaluated because the resection range was different in each case. Therefore, further studies with larger patient series and fully correlated pathological examinations are needed.

In conclusion, metastases to the parotid nodes tend to occur as solitary masses. Their preferential sites are the parotid tail or the pretragal area in the superficial lobe.

References

- Bradley PJ, McGurk M. Incidence of salivary gland neoplasms in a defined UK population. *Br J Oral Maxillofac Surg* 2013; **51**: 399–403. doi: <https://doi.org/10.1016/j.bjoms.2012.10.002>
- Eveson JW, Cawson RA. Salivary gland tumours. A review of 2410 cases with particular reference to histological types, site, age and sex distribution. *J Pathol* 1985; **146**: 51–8. doi: <https://doi.org/10.1002/path.1711460106>
- Tian Z, Li L, Wang L, Hu Y, Li J. Salivary gland neoplasms in oral and maxillofacial regions: a 23-year retrospective study of 6982 cases in an eastern Chinese population. *Int J Oral Maxillofac Surg* 2010; **39**: 235–42. doi: <https://doi.org/10.1016/j.ijom.2009.10.016>
- O'Hara J, Ferlito A, Takes RP, Rinaldo A, Strojjan P, Shaha AR, et al. Cutaneous squamous cell carcinoma of the head and neck metastasizing to the parotid gland—a review of current recommendations. *Head Neck* 2011; **33**: 1789–95. doi: <https://doi.org/10.1002/hed.21583>
- Garatea-Crelgo J, Gay-Escoda C, Bermejo B, Buenechea-Imaz R. Morphological study of the parotid lymph nodes. *J Craniomaxillofac Surg* 1993; **21**: 207–9.
- Hamilton BE, Salzman KL, Wiggins RH, Harnsberger HR. Earring lesions of the parotid tail. *AJNR Am J Neuroradiol* 2003; **24**: 1757–64.
- Malata CM, Camilleri IG, McLean NR, Piggott TA, Soames JV. Metastatic tumours of the parotid gland. *Br J Oral Maxillofac Surg* 1998; **36**: 190–5. doi: [https://doi.org/10.1016/S0266-4356\(98\)90496-X](https://doi.org/10.1016/S0266-4356(98)90496-X)
- Nuyens M, Schüpbach J, Stauffer E, Zbären P. Metastatic disease to the parotid gland. *Otolaryngol Head Neck Surg* 2006; **135**: 844–8. doi: <https://doi.org/10.1016/j.otohns.2006.05.010>
- Clark J, Wang S. Metastatic cancer to the parotid. *Adv Otorhinolaryngol* 2016; **78**: 95–103. doi: <https://doi.org/10.1159/000442129>
- Teymoortash A, Dünne AA, Werner JA. Parotid lymph node metastasis in squamous cell carcinoma of the skin. *Eur J Dermatol* 2002; **12**: 376–80.
- Thom JJ, Moore EJ, Price DL, Kasperbauer JL, Starkman SJ, Olsen KD. The role of total parotidectomy for metastatic cutaneous squamous cell carcinoma and malignant melanoma. *JAMA Otolaryngol Head Neck Surg* 2014; **40**: 548–54. doi: <https://doi.org/10.1001/jamaoto.2014.352>
- Lee YY, Wong KT, King AD, Ahuja AT. Imaging of salivary gland tumours. *Eur J Radiol* 2008; **66**: 419–36. doi: <https://doi.org/10.1016/j.ejrad.2008.01.027>
- Christe A, Waldherr C, Hallett R, Zbaeren P, Thoeny H. MR imaging of parotid tumors: typical lesion characteristics in MR imaging improve discrimination between benign and malignant disease. *AJNR Am J Neuroradiol* 2011; **32**: 1202–7. doi: <https://doi.org/10.3174/ajnr.A2520>
- Horii A, Yoshida J, Honjo Y, Mitani K, Takashima S, Kubo T. Pre-operative assessment of metastatic parotid tumors. *Auris Nasus Larynx* 1998; **25**: 277–83. doi: [https://doi.org/10.1016/S0385-8146\(97\)10041-4](https://doi.org/10.1016/S0385-8146(97)10041-4)
- Harada H, Omura K. Metastasis of oral cancer to the parotid node. *Eur J Surg Oncol* 2009; **35**: 890–4. doi: <https://doi.org/10.1016/j.ejso.2008.09.013>
- Pisani P, Ramponi A, Pia F. The deep parotid lymph nodes: an anatomical and oncological study. *J Laryngol Otol* 1996; **110**: 148–50. doi: <https://doi.org/10.1017/S0022215100133006>
- McKean ME, Lee K, McGregor IA. The distribution of lymph nodes in and around the parotid gland: an anatomical study. *Br J Plast Surg* 1985; **38**: 1–5. doi: [https://doi.org/10.1016/0007-1226\(85\)90078-5](https://doi.org/10.1016/0007-1226(85)90078-5)
- D'Souza J, Clark J. Management of the neck in metastatic cutaneous squamous cell carcinoma of the head and neck. *Curr Opin Otolaryngol Head Neck Surg* 2011; **19**: 99–105. doi: <https://doi.org/10.1097/MOO.0b013e328343e811>
- Vauterin TJ, Veness MJ, Morgan GJ, Poulsen MG, O'Brien CJ. Patterns of lymph node spread of cutaneous squamous cell carcinoma of the head and neck. *Head Neck* 2006; **28**: 785–9. doi: <https://doi.org/10.1002/hed.20417>
- Suton P, Lkšić I, Müller D, Virag M. Lymphatic drainage patterns of head and neck cutaneous melanoma: does primary melanoma site correlate with anatomic distribution of pathologically involved lymph nodes? *Int J Oral Maxillofac Surg* 2012; **41**: 413–20. doi: <https://doi.org/10.1016/j.ijom.2011.12.027>

21. Li XM, Wei WI, Guo XF, Yuen PW, Lam LK. Cervical lymph node metastatic patterns of squamous carcinomas in the upper aerodigestive tract. *J Laryngol Otol* 1996; **110**: 937–41. doi: <https://doi.org/10.1017/S0022215100135406>
22. Shah JP. Patterns of cervical lymph node metastasis from squamous carcinomas of the upper aerodigestive tract. *Am J Surg* 1990; **160**: 405–9. doi: [https://doi.org/10.1016/S0002-9610\(05\)80554-9](https://doi.org/10.1016/S0002-9610(05)80554-9)
23. Nam IC, Park JO, Joo YH, Cho KJ, Kim MS. Pattern and predictive factors of regional lymph node metastasis in papillary thyroid carcinoma: a prospective study. *Head Neck* 2013; **35**: 40–5. doi: <https://doi.org/10.1002/hed.22903>
24. Kimura Y, Sumi M, Sakihama N, Tanaka F, Takahashi H, Nakamura T. MR imaging criteria for the prediction of extranodal spread of metastatic cancer in the neck. *AJNR Am J Neuroradiol* 2008; **29**: 1355–9. doi: <https://doi.org/10.3174/ajnr.A1088>
25. Lodder WL, Lange CA, van Velthuysen ML, Hauptmann M, Balm AJ, van den Brekel MW, et al. Can extranodal spread in head and neck cancer be detected on MR imaging. *Oral Oncol* 2013; **46**: 626–33. doi: <https://doi.org/10.1016/j.oraloncology.2013.02.010>
26. Zoumalan RA, Kleinberger AJ, Morris LG, Ranade A, Yee H, DeLacure MD, et al. Lymph node central necrosis on computed tomography as predictor of extracapsular spread in metastatic head and neck squamous cell carcinoma: pilot study. *J Laryngol Otol* 2010; **12**: 1284–8. doi: <https://doi.org/10.1017/S0022215110001453>
27. Patel DK, Morton RP. Demographics of benign parotid tumours: Warthin's tumour *versus* other benign salivary tumours. *Acta Otolaryngol* 2016; **136**: 83–6. doi: <https://doi.org/10.3109/00016489.2015.1081276>
28. Ikeda M, Motoori K, Hanazawa T, Nagai Y, Yamamoto S, Ueda T, et al. Warthin tumor of the parotid gland: diagnostic value of MR imaging with histopathologic correlation. *AJNR Am J Neuroradiol* 2004; **25**: 1256–62.
29. Kato H, Kanematsu M, Watanabe H, Mizuta K, Aoki M. Salivary gland tumors of the parotid gland: CT and MR imaging findings with emphasis on intratumoral cystic components. *Neuroradiology* 2014; **56**: 789–95. doi: <https://doi.org/10.1007/s00234-014-1386-3>